

# Ultrashort-Pulse Cross Polarization Scattering in Plasmas with Magnetic Shear

HOJO Hitoshi\* and MASE Atsushi<sup>1</sup>

*Plasma Research Center, University of Tsukuba, Tsukuba 305-8577, Japan*

*<sup>1</sup>Advanced Science and Technology Center for Cooperative Research,  
Kyushu University, Kasuga 816-8580, Japan*

(Received: 19 January 2000 / Accepted: 18 April 2000)

## Abstract

The time-domain coupled equations being able to describe the cross polarization scattering of ultrashort-pulse electromagnetic waves in plasmas with magnetic shear are derived from Maxwell wave equation with equation of motion for the electron. The computational results on the cross polarization scattering induced by a magnetic fluctuation is also shown for an incident ordinary-mode pulse.

## Keywords:

cross polarization scattering, ultrashort-pulse, diagnostic, magnetic shear, Fidone-Granata's equation

## 1. Introduction

Microwave-based diagnostics such as reflectometry have received much attention as a nonperturbing diagnostic for probing plasma profiles and fluctuations in magnetically confined plasmas. Recently, the cross polarization scattering phenomena of microwaves were observed in GAMMA 10 [1] and the Tore Supra Tokamak [2]. Since the cross polarization scattering between ordinary and extraordinary waves is caused by magnetic fluctuations or magnetic shear, it is applicable to probing magnetic fluctuations and also to measuring magnetic shear profiles in magnetic confinement devices. Particularly, since ultrashort-pulse electromagnetic waves can be considered as a set of many monochromatic continuous waves with different frequencies, the microwave diagnostic using ultrashort-pulse waves can possess the advantage that the reflected or transmitted waves carry large amounts of information of a plasma such as fluctuations, compared to a monochromatic continuous wave [3-7]. This is useful not only for a pulsed plasma such as tokamak but a steady plasma such as helical system and mirror.

In this paper, we consider the cross polarization scattering of ultrashort-pulse electromagnetic waves in a magnetically confined plasma. In the following section, we derive the time-domain wave equation being able to describe the cross polarization scattering of ultrashort-pulse electromagnetic waves in a plasma with magnetic shear. The derived equation just becomes a time-domain formalism of the usual Fidone-Granata's equation [8]. In section 3, we show the computational results on the cross polarization scattering of ultrashort-pulse electromagnetic waves induced by magnetic fluctuations.

## 2. Time-Domain Fidone-Granata's equation

In this section, we derive the time-domain wave equation being able to describe the cross polarization scattering of ultrashort-pulse electromagnetic waves in plasmas with magnetic shear. For simplicity, we here discuss one-dimensional propagation of ordinary (O) and extraordinary (X) modes in  $(x,t)$  space. The starting point is the linearized wave equations describing the O and X modes given by

\*Corresponding author's e-mail: hojo@prc.tsukuba.ac.jp

$$\left(\frac{\partial^2}{\partial t^2} + c^2 \nabla \times \nabla \times\right) \mathbf{E} + \frac{1}{\epsilon_0} \frac{\partial}{\partial t} \mathbf{J} = 0 \quad (1)$$

$$\frac{1}{\epsilon_0} \frac{\partial}{\partial t} \mathbf{J} = \omega_{pe}^2 \mathbf{E} + \frac{1}{\epsilon_0} \omega_{ce} \mathbf{J} \times \frac{\mathbf{B}_0}{B_0} \quad (2)$$

where  $\mathbf{B}_0(x) = B_z \hat{z} + B_y \hat{y}$  is an external magnetic field,  $\omega_{pe}(= \sqrt{e^2 n_0 / \epsilon_0 m_e})$  the electron plasma frequency and  $\omega_{ce}(= -e B_0 / m_e)$  the electron cyclotron frequency. Here in deriving eq. (2), we assume that the current density is approximated as  $\mathbf{J} = -en_0 \mathbf{v}_e$ , with  $\mathbf{v}_e$  being electron flow velocity, when we consider electromagnetic waves in the GHz range.

From eqs. (1) and (2), we obtain, for  $E_x$ ,  $E_y$  and  $E_z$ ,

$$\left(\frac{\partial^2}{\partial t^2} + \omega_{pe}^2 + \omega_{ce}^2\right) \frac{\partial}{\partial t} E_x + \omega_{pe}^2 \omega_{ce} (b_z E_y - b_y E_z) = 0, \quad (3)$$

$$\left(\frac{\partial^2}{\partial t^2} - c^2 \frac{\partial^2}{\partial x^2} + \omega_{pe}^2\right) E_y + \omega_{ce} b_z \frac{\partial}{\partial t} E_x = 0, \quad (4)$$

$$\left(\frac{\partial^2}{\partial t^2} - c^2 \frac{\partial^2}{\partial x^2} + \omega_{pe}^2\right) E_z - \omega_{ce} b_y \frac{\partial}{\partial t} E_x = 0, \quad (5)$$

where  $b_y = B_y / B_0$  and  $b_z = B_z / B_0$ . If we here introduce the wave electric field  $E_\perp$  and  $E_\parallel$  (perpendicular and parallel to  $\mathbf{B}_0$ , respectively) given by

$$\begin{pmatrix} E_\perp \\ E_\parallel \end{pmatrix} = \begin{pmatrix} \cos \theta & -\sin \theta \\ \sin \theta & \cos \theta \end{pmatrix} \begin{pmatrix} E_y \\ E_z \end{pmatrix} \quad (6)$$

with  $b_y = \sin \theta$  and  $b_z = \cos \theta$ , we obtain, from eqs. (4) and (5),

$$\sin \theta \hat{L} E_\parallel + \cos \theta \hat{L} E_\perp - c^2 \cos \theta (2E_\parallel' \theta' + E_\parallel \theta'') + c^2 \sin \theta (2E_\perp' + E_\perp \theta'') + \omega_{ce} \cos \theta \partial E_x / \partial t = 0 \quad (7)$$

$$\cos \theta \hat{L} E_\parallel - \sin \theta \hat{L} E_\perp + c^2 \sin \theta (2E_\parallel' \theta' + E_\parallel \theta'') + c^2 \cos \theta (2E_\perp' + E_\perp \theta'') - \omega_{ce} \sin \theta \partial E_x / \partial t = 0 \quad (8)$$

with

$$\hat{L} = \frac{\partial^2}{\partial t^2} - c^2 \frac{\partial^2}{\partial x^2} + \omega_{pe}^2 + c^2 \theta'^2,$$

where  $\theta = \arctan(b_y / b_z)$  and the symbol ' denotes the derivative with respect to  $x$ .

Using eqs. (7) and (8), we finally obtain the coupled wave equations for  $E_\parallel$ ,  $E_\perp$  and  $E_x$  given by

$$\left(\frac{\partial^2}{\partial t^2} - c^2 \frac{\partial^2}{\partial x^2} + \omega_{pe}^2 + c^2 \theta'^2\right) E_\parallel = -c^2 \left(2 \frac{\partial E_\perp}{\partial x} \theta' + E_\perp \theta''\right) \quad (9)$$

$$\left(\frac{\partial^2}{\partial t^2} - c^2 \frac{\partial^2}{\partial x^2} + \omega_{pe}^2 + c^2 \theta'^2\right) E_\perp + \omega_{ce}^2 \frac{\partial}{\partial t} E_x = c^2 \left(2 \frac{\partial E_\parallel}{\partial x} \theta' + E_\parallel \theta''\right) \quad (10)$$

$$\left(\frac{\partial^2}{\partial t^2} + \omega_{pe}^2 + \omega_{ce}^2\right) \frac{\partial}{\partial t} E_x + \omega_{pe}^2 \omega_{ce} E_\perp = 0. \quad (11)$$

The above coupled equations are the time-domain wave equations being able to describe the cross polarization scattering of ultrashort-pulse O and X modes. From eqs. (9) and (10), we see that the magnetic shear effects  $\theta'$  and  $\theta''$  induce the cross polarization scattering between O( $E_\parallel$ ) and X( $E_\perp$ ,  $E_x$ ) modes. Even though low-frequency magnetic fluctuation  $\delta \mathbf{B}$  with its frequency much smaller than GHz exists, the above equations still hold if  $\mathbf{B}_0$  is replaced by  $\mathbf{B}_0 + \delta \mathbf{B}$ . Therefore, the above equations can also describe the cross polarization scattering induced by magnetic fluctuations.

For stationary continuous wave propagation, if we put  $E \sim \exp(-i\omega t)$ , we can obtain the usual Fidone-Granata's equation [8] given by

$$\left[\frac{d^2}{dx^2} + \frac{\omega^2}{c^2} \left(1 - \frac{\omega_{pe}^2}{\omega^2}\right) - \theta'^2\right] E_\parallel = 2 \frac{dE_\perp}{dx} \theta' + E_\perp \theta'' \quad (12)$$

$$\left[\frac{d^2}{dx^2} + \frac{\omega^2}{c^2} \left(1 - \frac{\omega_{pe}^2}{\omega^2} \frac{\omega^2 - \omega_{pe}^2}{\omega^2 - \omega_{uh}^2}\right) - \theta'^2\right] E_\perp = -2 \frac{dE_\parallel}{dx} \theta' - E_\parallel \theta'' \quad (13)$$

where  $\omega_{uh}(= \sqrt{\omega_{pe}^2 + \omega_{ce}^2})$  is the upper-hybrid frequency.

### 3. Computational Results

In this section, We show the computational results of eqs. (1) and (2) on the cross polarization scattering of ultrashort-pulse O and X modes. We here assume a uniform magnetic field  $\mathbf{B}_0$  in order to study the cross polarization scattering induced by magnetic fluctuation.

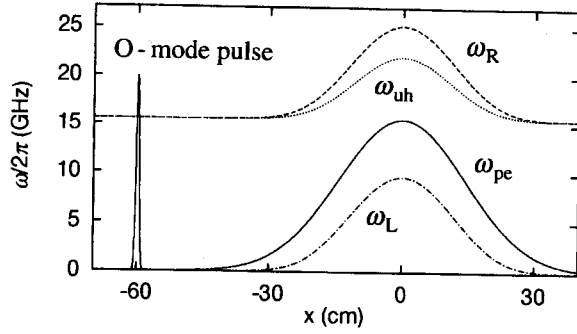


Fig. 1 The schematic view of the computational model, where the incident o-mode pulse is located at  $x = -60$  cm and the profiles of several characteristic frequencies are also shown.

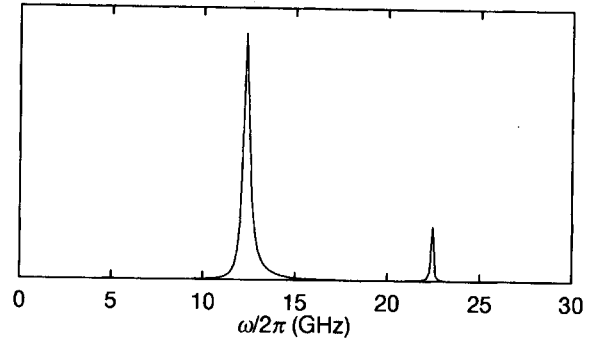


Fig. 2 The frequency-spectral signal of the mode-converted X mode observed at  $x = -60$  cm by MEM.

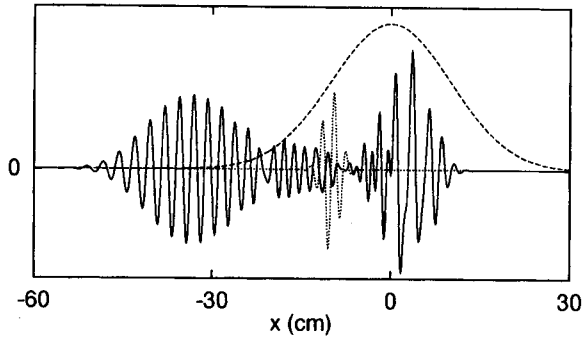


Fig. 3 The profiles of the mode-converted X mode (solid line), density profile (dashed line) and magnetic fluctuation (dotted line).

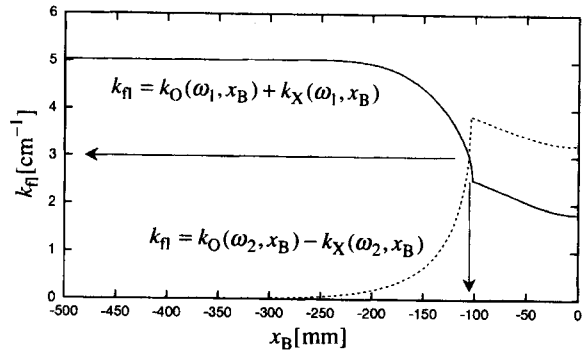


Fig. 4 The wave number and localization position  $x_B$  of the magnetic fluctuation are obtained from two Bragg resonance conditions  $k_\eta = k_O + k_X$  and  $k_\eta = k_O - k_X$ .

The assumed model shown in Fig. 1 is as follows: We assume a Gaussian density profile given by  $n_0(x) = N_0 \exp(-x^2/L^2)$  with  $N_0 = 3 \times 10^{12} \text{ cm}^{-3}$ ,  $L = 20$  cm and  $|\omega_{ce}| = \omega_{pe}(x = 0)$ . In Fig. 1, the profiles of the right-hand cutoff  $\omega_R$  (dashed line), the upper-hybrid frequency  $\omega_{uh}$  (dotted line),  $\omega_{pe}$  (solid line) and the left-hand cutoff  $\omega_L$  (chained line) are shown. The incident wave is an O-mode ( $E_{||}$ ) pulse located at  $x = x_0 = -60$  cm with the waveform of  $E_z(x, t = 0) = E_0 \exp[-(x - x_0)^2/L_p^2]$  with  $L_p = 0.5$  cm. The incident pulse width  $\tau_p (= 2 L_p/c)$  is about 33 ps and  $1/\tau_p$  exceeds the maximum of  $\omega_R/2\pi$ . The incident pulse is also shown by a solid line in Fig. 1. For a magnetic fluctuation ( $\delta B = \hat{B}\phi$ ), we assume the waveform  $\hat{B}(x) = B_f \exp[-(x - x_B)^2/L_B^2] \sin[k_B(x - x_B)]$  with  $L_B = 2$  cm,  $k_B = 3 \text{ cm}^{-1}$  and  $x_B = -10$  cm, where  $B_f$  is the amplitude of a magnetic fluctuation. We numerically solve eqs. (1) and (2) using a finite difference scheme.

In Fig. 2, we show the frequency-spectral signal of the mode-converted X mode ( $E_{\perp}$ ) that is reflected and

received at  $x = -60$  cm by the maximum entropy method (MEM). We find that two peaks exist in the spectral signal and the peak frequencies are 12.4 GHz and 22.5 GHz. In Fig. 3, we show the wave pattern (solid line) of the mode-converted X mode at  $t = 4$  ns, the magnetic fluctuation (dotted line) and density (dashed line) profiles.

We hereafter show that the above spectral signal is due to the cross polarization scattering between O and X modes induced by the magnetic fluctuation. We now consider the magnetic fluctuation to be approximately a wave with zero frequency and the wave number of  $k_\eta = k_B$  and assume the local dispersion relations for O and X modes. In this case, we have two Bragg resonance conditions in the wave number among O and X modes and the magnetic fluctuation, given by

$$k_O(\omega_1, x_B) - k_\eta = -k_X(\omega_1, x_B), \quad (14)$$

$$k_O(\omega_2, x_B) - k_{\parallel} = -k_X(\omega_2, x_B), \quad (15)$$

where  $k_O$  and  $k_X$  are the local wave numbers of O and X modes, respectively. If we substitute  $k_{\parallel} = k_B = 3 \text{ cm}^{-1}$  and  $x_B = -10 \text{ cm}$  into eqs. (14) and (15), we obtain  $\omega_1/2\pi \cong 12.3 \text{ GHz}$  and  $\omega_2/2\pi \cong 22.3 \text{ GHz}$ . We see that these values are very close to the observed peak frequencies, 12.4GHz and 22.5GHz, shown in Fig. 2. Therefore, we can conclude that the cross polarization scattering processes characterized by the Bragg resonance of eqs. (14) and (15) take place in the simulation. Adversely, if we substitute  $\omega_1/2\pi \cong 12.4 \text{ GHz}$  and  $\omega_2/2\pi \cong 22.5 \text{ GHz}$  into eqs. (14) and (15), we can obtain  $k_{\parallel} \cong 3 \text{ cm}^{-1}$  and  $x_B \cong 10 \text{ cm}$  by solving eqs. (14) and (15) for  $k_{\parallel}$  and  $x_B$  as shown in Fig. 4, where the solid and dotted lines denote  $k_{\parallel} = k_O + k_X$  of eq. (14) and  $k_{\parallel} = k_O - k_X$  of eq. (15), respectively. This shows that we can find the wave number and localization position of the magnetic fluctuation from observed frequency-spectral data of the mode-converted X mode, when the Bragg resonance condition is well defined for magnetic fluctuations.

Finally, the computational study on reconstructing magnetic profiles with shear and also probing magnetic fluctuations based on the time-domain Fidone-Granata's equation will be reported in future.

### Acknowledgement

This work was partly supported by a Grant-in-Aid for Scientific Research from the Ministry of Education, Science, Sports and Culture of Japan.

### References

- [1] A. Mase, T. Tokuzawa, N. Oyama, Y. Ito, A. Itakura, H. Hojo, M. Ichimura and T. Tamano, *Rev. Sci. Instrum.* **66**, 821 (1995).
- [2] X.L. Zou, L. Colas, M. Paume, J.M. Chareau, L. Laurent, P. Devynck and D. Gresillon, *Phys. Rev. Lett.* **75**, 1090 (1995).
- [3] C.W. Domier, N.C. Luhmann, Jr., A.E. Chou, W.M. Zhang and A.J. Romanowski, *Rev. Sci. Instrum.* **66**, 399 (1995).
- [4] S. Kubota, T. Onuma, A. Mase, T. Tokuzawa, N. Oyama, A. Itakura, H. Hojo, L. Bruskin, T. Tamano, K. Yatsu, C. Domier and N. Luhmann, Jr., *Jpn. J. Appl. Phys.* **37**, L300 (1998).
- [5] N. Katsuragawa, H. Hojo and A. Mase, *J. Phys. Soc. Jpn.* **67**, 2574 (1998).
- [6] H. Hojo, Y. Kurosawa and A. Mase, *Rev. Sci. Instrum.* **70**, 983 (1999).
- [7] B.I. Cohen, E.B. Hooper, T.B. Kaiser, E.A. Williams and C.W. Domier, *Phys. Plasmas* **6**, 1732 (1999).
- [8] I. Fidone and G. Granata, *Nucl. Fusion* **11**, 133 (1971).